Journal of Mathematical Modeling
Vol. 8, No. 3, 2020, pp. 291–308

JMM

The method of lines for parabolic integro-differential equations

Samaneh Soradi-Zeid[†*] **, Mehdi Mesrizadeh**[‡]

[†]*Faculty of Industry and Mining (Khash), University of Sistan and Baluchestan, Zahedan, Iran*
[‡]*Department of Mathematics, Imam Khomeini International University, Qazvin, Iran*

Email(s): soradizeid@eng.usb.ac.ir, mehdi.mesrizadeh@yahoo.com

Abstract. This paper introduces an efficient numerical scheme for solving a significant class of nonlinear parabolic integro-differential equations (PIDEs). The major contributions made in this paper are applying a direct approach based on a combination of group preserving scheme (GPS) and spectral meshless radial point interpolation (SMRPI) method to transcribe the partial differential problem under study into a system of ordinary differential equations (ODEs). The resulting problem is then solved by employing the numerical method of lines, which is also a well-developed numerical method. Two numerical experiments are carried out to evaluate the performance and effectiveness of the suggested framework.

Keywords: Parabolic integro-differential equation, partial differential equation, meshless method, radial point interpolation technique, group preserving scheme.
AMS Subject Classification 2010: 26A33, 45J05, 34K10.

1 Introduction

Consider the following PIDE:

$$\mathbf{y}_t(t,\mathbf{x}) - \nabla \cdot \mathbf{p}(t,\mathbf{x}) = \mathbf{f}(t,\mathbf{x}), \quad (\mathbf{x},t) \in \Omega \times (0,T], \tag{1}$$

*Corresponding author.
Received: 7 March 2020 / Revised: 6 May 2020 / Accepted: 6 May 2020.
DOI: 10.22124/jmm.2020.15954.1397

where

$$\mathbf{p}(t,\mathbf{x}) = \mathbf{A}(t,\mathbf{x})\nabla\mathbf{y}(t,\mathbf{x}) - \int_0^t \mathbf{B}(t,s,\mathbf{x})\nabla\mathbf{y}(s,\mathbf{x})ds,$$

with the initial and boundary conditions

$$\begin{aligned} &\mathbf{y}(t,\mathbf{x}) = 0, && (\mathbf{x},t) \in \partial\Omega \times (0,T], \\ &\mathbf{y}(0,\mathbf{x}) = g(\mathbf{x}), && \mathbf{x} \in \Omega, \end{aligned}$$

in which $\Omega \subseteq \mathbb{R}^d$, $d = 2, 3$, is a bounded polygonal domain with the boundary $\partial\Omega$, $\mathbf{A}$ and $\mathbf{B}$ are two $d \times d$ matrices, $\mathbf{f}$ is a given real-valued function on Ω and $g(\mathbf{x})$ is a known function.

This issue have been used through modeling many nonlinear physical applications evidently. More specifically, PIDEs used to illustrate the mechanics and dynamic systems [4, 12, 14, 32, 34]. Nonetheless it should be noted that due to the high complexity of parabolic and nonlinear partial differential equations, the analytically handling equations portrayed by this nonlinearity is completely tough and even impossible. To be prevailed through this challenge, practical numerical/approximate methods have been presenting to solve them [10, 17]. Authors in [35], utilized compact difference approach for spatial discretization and alternating direction implicit method in time, combined with second-order fractional quadrature rule for the approximating of integral term to solve a class of PIDEs with weakly singular kernels in which the existence of positive solutions of this problem had already been interrogated by Chen and Zou [8]. The two-grid finite element algorithm is expanded by Wang and Hong in [44] for solving problem (1) with nonlinear memory. Because of the high efficiency of nonlinear term in the problem (1), this discretization results in highly nonlinear algebraic systems. To overcome this challenge, the researcher used a linearized iterative process that vividly cause the numerical results have much computational error. Through the next year, Deka et al. [9] developed this method but the reported numerical results weren't better than previously reported results. Reddy et al. [36] have used the Crank-Nicolson finite element techniques in order to perform an improved a posteriori error analysis for the PIDEs with a bounded convex polygonal or polyhedral domain. Also, a compact difference approach for spatial discretization and alternating direction implicit method in time, combined with second-order fractional quadrature rule has been investigated in [35]. An investigation on a class of quasilinear PIDEs with nonlinear boundary conditions has been proposed in [47]. Other methods used to solve different types of this problems include finite element method [5, 11, 20, 28, 33, 46] and

finite difference method [16, 27, 43]. Recently, several new numerical methods such as mixed finite element method and finite volume element method for space discretization or time discretization have been proposed to solve PIDEs [3,7,21,30,37,38]. Many meshless methods, as a special class of spectral methods, have been used for solving the PIDE such as the Galerkin method [18, 19, 31] Galerkin finite element scheme [48]. On the contrary of easy implementation of these methods, the challenge of these methods is their low accuracy and high cost of computing in discretization. Different from these techniques, here the parabolic equation (1) is discretized directly into nonlinear algebraic system by the method of lines. Besides, to deal with the nonlinearity, two iterative procedures are developed.

SMRPI method, comprised of meshless radial point interpolation and spectral collocation techniques, has been assigned and applied to the 2-D and 3-D diffusion equations by Shivanian in [39–42]. Through this technique, the point interpolation method with the help of radial basis functions (RBFs) is proposed to implement basis functions which have Kronecker delta function property and are used as basis functions in the frame of the SMRPI. The given method either utilize any global basis functions for interpolating technique or uses arbitrary points for discretization, give us a very flexible chart for solving PIDEs. Using SMRPI as a meshless collocation method bears some advantages sush as simply evaluation of high order derivatives of given differential equation and less expensive of computational costs.

In this study, based on the numerical method of lines, which is also a well-developed numerical method, a semi-discretization is implemented on the state variable of PIDE (1) by SMRPI method to obtain a system of ODEs. After that, a highly accurate and powerful approximate scheme namlely the GPS suitable for ODEs is employed to acquire the approximate solution of this system. The GPS is a robust method used to solve some different problems such as Klein-Gordon model [13], telegraph equation [15], Sturm-Liouville problem [26], Burgers equation [22,23], Bratu problem [1], heat conduction problem [6, 24] and the Cauchy Problem [2, 13]. The GPS, as a geometric method, is formed in the Minkowski space $\mathbb{M}^{n+1}$, whereas the traditional numerical approaches (non-geometric methods) are all formulated directly in the usual Euclidean space $\mathbb{R}^n$. Avoiding the spurious solutions and ghost fixed points is one of the benefits of using the augmented Minkowski space as a Lie group.

So, the overall layout of this paper is as follows. Section 2, is relevant to some properties of the GPS and SMRPI method in short. Section 3, is committed to the PIDE under study and its approximation by means of the

mentioned functions. According to the existing mechanism, the synchronization problem is recast to a system of ODEs. Section 4, is dedicated to the simulation results. The experimental results demonstrate the validity and capability of the proposed computational procedure. In Section 5, we provide a conclusion.

2 Preliminaries

In this section, a brief description of GPS for solving a system of ODEs and some of the stability results of this method is presented. Furthermore, the SMRPI method and some of its properties are derived. Also, a new and applied feature in nonlinear issues is expressed for it.

2.1 Group Preserving Scheme

We introduce the GPS, which was firstly derived by Liu [25]. GPS uses the Cayley transformation and the Pade$'$ approximations in the augmented space, namely Minkowski. Consider a system of n ordinary differential equations:

$$\mathbf{u}'(x) = \mathbf{f}(\mathbf{u}(x), x), \quad x \in \mathbb{R}, \quad \mathbf{u}(x) \in \mathbb{R}^n, \tag{2}$$

where $\mathbf{f}$ is a vector valued function. Assume that $\|\mathbf{u}(x)\| > 0$ in which $\|.\|$ is the Euclidean norm. So, the dynamical system (2) can be transformed as following:

$$\frac{d}{dx}\begin{pmatrix}\mathbf{u}(x)\\ \|\mathbf{u}(x)\|\end{pmatrix} = \begin{pmatrix}\mathbf{0}_{n\times n} & \frac{\mathbf{f}(\mathbf{u}(x),x)}{\|\mathbf{u}(x)\|}\\ \frac{\mathbf{f}^T(\mathbf{u}(x),x)}{\|\mathbf{u}(x)\|} & 0\end{pmatrix}\begin{pmatrix}\mathbf{u}(x)\\ \|\mathbf{u}(x)\|\end{pmatrix}. \tag{3}$$

Let us put the Minkowski metric as follows

$$\mathbf{g} = \begin{pmatrix}\mathbf{I}_n & \mathbf{0}_{n\times 1}\\ \mathbf{0}_{1\times n} & \mathbf{I}_n\end{pmatrix},$$

where $\mathbf{I}_n$ is the identity matrix and

$$\mathbf{U}(x) = \begin{pmatrix}\mathbf{u}(x)\\ \|\mathbf{u}(x)\|\end{pmatrix}.$$

One can easily show that the augmented state variables of $U(x)$ satisfies the following cone condition

$$\mathbf{U}^T(x)\mathbf{g}\mathbf{U}(x) = \mathbf{u}^T(x).\mathbf{u}(x) - \|\mathbf{u}(x)\|^2 = 0, \quad \forall x \in \mathbb{R}. \tag{4}$$

From augmented technique, each equation of dynamical system (2) can be displayed on augmented dynamical system (3) that its solution is placed on the cone by the criterion (4). Moreover, the addition of the second equation of (3) imposes a Minkowski structure that acquiescent to (4). Briefly, the equation (3) can be written as the following

$$\mathbf{U}' = \mathbb{A}\mathbf{U}, \tag{5}$$

in which

$$\mathbb{A}(\mathbf{u}(x), x) = \begin{pmatrix} \mathbf{0}_{n\times n} & \frac{\mathbf{f}(\mathbf{u}(x),x)}{\|\mathbf{u}(x)\|} \\ \frac{\mathbf{f}^T(\mathbf{u}(x),x)}{\|\mathbf{u}(x)\|} & 0 \end{pmatrix},$$

and the augmented matrix $\mathbb{A}$ that satisfies

$$\mathbb{A}^T\mathbf{g} + \mathbf{g}\mathbb{A} = 0, \tag{6}$$

is also an element of the Lie algebra $\mathfrak{so}(n,1)$ of the proper orthochronous Lorentz group $SO_\circ(n,1)$ for all $x \in \mathbb{R}$. Although the dimension of the new system (5) is raising one more that system (2), it has been shown that under the Lipschitz condition for f, this new system has the advantage of allowing us to develop the GP numerical scheme. The GPS is developed by Liu [25] that each $\mathbf{U}_k$ being numerical value of $\mathbf{U}(x_k)$ can automatically locate on the cone

$$\mathbf{U}_{k+1} = \mathbb{G}_k\mathbf{U}_k, \tag{7}$$

in which the cone condition can be constrained on $\mathbf{U}_k$'s as following

$$\mathbf{U}_k\mathbf{g}\mathbf{U}_k = 0, \quad \text{for} \quad k = 0, 1, 2, \ldots, \tag{8}$$

where $\mathbb{G}_k \in SO_\circ(n,1)$, $\forall k$, are verified to satisfy the following properties:

$$\mathbb{G}_k^T\mathbf{g}\mathbb{G}_k = \mathbf{g}, \tag{9}$$

$$\det \mathbb{G}_k = 1, \tag{10}$$

$$\mathbb{G}_k^{00} > 0, \tag{11}$$

where $\mathbb{G}_k^{00}$ is 00-th component of the matrix $\mathbb{G}_k$. The k-th stage of one-step differential equation system with the initial condition $\mathbf{U}_k$ on the interval $[x_k, x_{k+1}]$ has the following form:

$$\begin{aligned} \mathbf{U}'(x) &= \mathbb{A}(\mathbf{U}(x), x)\mathbf{U}(x), \quad x \in (x_k, x_{k+1}], \\ \mathbf{U}(x_k) &= \mathbf{U}_k. \end{aligned} \tag{12}$$

The exact solution of (12) is computed as

$$\mathbf{U}(x) = e^{\int_{x_k}^{x} \mathbb{A}(\mathbf{U}(t),t)dt}\mathbf{U}_k, \quad x \in (x_k, x_{k+1}], \tag{13}$$

In a special way, we rewrite the above equation for $x = x_{k+1}$, then we have:

$$\mathbf{U}(x_{k+1}) = e^{\int_{x_k}^{x_{k+1}} \mathbb{A}(\mathbf{U}(t),t)dt}\mathbf{U}_k. \tag{14}$$

Numerical solution of (14) can be obtained as follows

$$\mathbf{U}_{k+1} = e^{\Delta x \mathbb{A}(\mathbf{U}_k,x_k)}\mathbf{U}_k, \tag{15}$$

which has the following truncation error:

$$\begin{aligned}\mathbf{U}(x_{k+1}) - \mathbf{U}_{k+1} &= \big(e^{\int_{x_k}^{x_{k+1}} \mathbb{A}(\mathbf{U}(t),t)dt} - e^{\Delta x \mathbb{A}(\mathbf{U}_k,x_k)}\big)\mathbf{U}_k \\ &= \big(e^{\int_{x_k}^{x_{k+1}} \mathbb{A}(\mathbf{U}(t),t)dt - \Delta x \mathbb{A}(\mathbf{U}_k,x_k)} - \mathbf{I}_{n+1}\big)e^{\Delta x \mathbb{A}(\mathbf{U}_k,x_k)}\mathbf{U}_k \\ &= \mathbf{O}(\Delta x)e^{\Delta x \mathbb{A}(\mathbf{U}_k,x_k)}\mathbf{U}_k.\end{aligned} \tag{16}$$

We know that $\mathbb{A}(\mathbf{u}(x), x) \in \mathfrak{so}(n,1)$, accordingly, $\mathbb{A}(\mathbf{U}_k, x_k) \in SO_\circ(n,1)$, therefore by the inductive processing, if $\mathbf{U}_k$ satisfies the cone condition, then $\mathbf{U}_{k+1}$ is truest on it. A GPS is introduced for this purpose to preserves the cone condition such as the problem (3). We now present the closed-form representation of the appeared matrices on the any step of this scheme as follows [25]:

$$e^{\Delta x \mathbb{A}(\mathbf{U}_k,x_k)} = \begin{pmatrix} \mathbf{I}_n + \frac{(\alpha_k - 1)\mathbf{f}_k\mathbf{f}_k^T}{\|\mathbf{f}_k\|^2} & \frac{\beta_k \mathbf{f}_k}{\|\mathbf{f}_k\|} \\ \frac{\beta_k \mathbf{f}_k^T}{\|\mathbf{f}_k\|} & \alpha_k \end{pmatrix}, \tag{17}$$

where

$$\alpha_k = \cosh(\Delta x \frac{\|\mathbf{f}_k\|}{\|\mathbf{u}_k\|}), \quad \beta_k = \sinh(\Delta x \frac{\|\mathbf{f}_k\|}{\|\mathbf{u}_k\|}),$$

and $\mathbf{f}_k = \mathbf{f}(\mathbf{U}_k, x_k)$. Taking the first n-component of $\mathbf{U}_k$, for all $k = 1, 2, 3, \ldots$, and applying them for a practical numerical calculation that it is a one-step method, we obtain [1, 2]:

$$\mathbf{u}_{k+1} = \mathbf{u}_k + \eta_k \mathbf{f}_k, \tag{18}$$

where

$$\eta_k = \frac{(\alpha_k - 1)\mathbf{f}_k^T.\mathbf{u}_k + \beta_k \|\mathbf{u}_k\|\|\mathbf{f}_k\|}{\|\mathbf{f}_k\|^2}.$$

The iterative algorithm (18) is alike the forward one-step Euler method, but it is modified to satisfy the cone condition. A linear stability of the one-step method (18) is surveyed to end the current section. The definition of the linear stability, which was previously stated for a multi-step finite difference method [29], can be modified for a multi-step GPS. In addition, one can see the relationship between it and the other types of stability.

Definition 1. A multi-step scheme for each system of ODE with constant coefficient has a linear stability if and only if all complex eigenvalues of its coefficients matrix have a negative real parts.

The linear stability of method (18) is shown in the following theorem.

Theorem 1. *The one-step method* (18) *has linear stability.*

Proof. Consider $\mathbf{f}(\mathbf{u}(x), x) = \mathbf{A}\mathbf{u}(x)$ with the initial condition $\mathbf{u}(0) = \mathbf{u}_\circ$ that all of the eigenvalues of $\mathbf{A}$ have the negative real part. From (18), we have

$$\mathbf{u}_{k+1} = \big(\mathbf{I}_n + \eta_k \mathbf{A}\big)\mathbf{u}_k, \quad \text{for } k = 1, 2, 3, \ldots. \tag{19}$$

From the above equation, we conclude that

$$\mathbf{u}_{k+1} = \prod_{i=1}^{k} \big(\mathbf{I}_n + \eta_i \mathbf{A}\big)\mathbf{u}_\circ, \quad \text{for } k = 1, 2, 3, \ldots. \tag{20}$$

We know that $-\|\mathbf{u}_k\|\|\mathbf{f}_k\| \le \mathbf{u}_k.\mathbf{f}_k \le \|\mathbf{u}_k\|\|\mathbf{f}_k\|$, then [2]:

$$\frac{\|\mathbf{u}_k\|}{\|\mathbf{f}_k\|}\big(1 - e^{-\Delta x \frac{\|\mathbf{f}_k\|}{\|\mathbf{u}_k\|}}\big) \le \eta_k \le \frac{\|\mathbf{u}_k\|}{\|\mathbf{f}_k\|}\big(e^{\Delta x \frac{\|\mathbf{f}_k\|}{\|\mathbf{u}_k\|}} - 1\big). \tag{21}$$

Selecting Δx in the interval $(0, \frac{1}{\|\mathbf{A}\|})$ results in $\eta_k \approx \Delta x$, $\sum_{i=1}^{k} \eta_k \approx x_k$ and $\mathbf{I}_n + \eta_i \mathbf{A} \approx e^{\eta_i \mathbf{A}}$ (see [29]). Then, from (20) we conclude that

$$\mathbf{u}_{k+1} \approx e^{x_{k+1}\mathbf{A}}\mathbf{u}_\circ, \text{ for } k = 1, 2, 3, \ldots, \tag{22}$$

in which causes $\|\mathbf{u}_k\| \to 0$ as $k \to \infty$, since as we assumed that all of the eigenvalues of $\mathbf{A}$ have the negative real part. □

2.2 SMRPI scheme

To approximate the continuous function $u(\mathbf{x})$ we can use a localized meshless radial point interpolation called SMRPI method [40]. We briefly introduce it in this section. The continuous function $u(\mathbf{x})$ can be represented

via both RBFs $\mathbf{R}_i(\mathbf{x})$ and monomials in interest point $x \in \Omega_l$. So, the coefficients a_i and b_j can be considered as

$$u(\mathbf{x}) = \sum_{i=1}^{n} R_i(\mathbf{x})a_i + \sum_{j=1}^{m} P_j(\mathbf{x})b_j = \mathbf{R}^T(\mathbf{x})\mathbf{a} + \mathbf{P}^T(\mathbf{x})\mathbf{b}, \tag{23}$$

in which Ω_l is a disk centered at x_l with radius r_s, n is the number of point in Ω_l and m is the number of polynomial basis functions. When $m = 0$, only RBFs are used, otherwise, the RBF is augmented with m polynomial basis functions. In the point of interest x_l, we enforce Eq. (23) to be satisfied at those n nodes surrounding it. Then the linear algebraic equations system (23) is represented as follows:

$$\mathbf{U}_s = \mathbf{R}_n^T\mathbf{a} + \mathbf{P}_m^T\mathbf{b}, \tag{24}$$

in which $\mathbf{U}_s$ is the vector of function values defined as

$$\mathbf{U}_s = \{u_1, u_2, u_3, \ldots, u_n\}^T, \tag{25}$$

$\mathbf{R}_n$ denotes the RBFs moment matrix as follows

$$\mathbf{R}_n = \begin{pmatrix} \mathbf{R}_{1,1} & \mathbf{R}_{1,2} & \cdots & \mathbf{R}_{1,n} \\ \vdots & \vdots & \ddots & \vdots \\ \mathbf{R}_{n,1} & \mathbf{R}_{n,2} & \cdots & \mathbf{R}_{n,n} \end{pmatrix}, \tag{26}$$

and $\mathbf{P}_m$ which represents the polynomial moment matrix is defined as below

$$\mathbf{P}_m = \begin{pmatrix} p_1(\mathbf{x}_1) & p_1(\mathbf{x}_2) & \cdots, & p_1(\mathbf{x}_n) \\ \vdots & \vdots & \ddots & \vdots \\ p_m(\mathbf{x}_1) & p_m(\mathbf{x}_2) & \cdots, & p_m(\mathbf{x}_n) \end{pmatrix}. \tag{27}$$

Also, the vector of unknown coefficients for RBFs is

$$\mathbf{a} = \{a_1, a_2, a_3, \ldots, a_n\}^T, \tag{28}$$

and the vector of unknown coefficients for basis polynomial is

$$\mathbf{b} = \{b_1, b_2, b_3, \ldots, b_m\}^T. \tag{29}$$

Assume that r_k, $k = 1, 2, \ldots, n$, being the distance between nodes in the support domain, $\mathbf{R}_{k,i} = \mathbf{R}_i(r_k)$ are the RBFs in (26). We added the following m equations in (24) to make a square matrix:

$$\sum_{i=1}^{n} p_j(\mathbf{x}_i)a_i = \mathbf{P}_m^T\mathbf{a} = 0, \quad j = 1, 2, \ldots, m. \tag{30}$$

So, the following system of equations is obtained from Eqs. (24) and (30):

$$\hat{\mathbf{U}}_s = \begin{pmatrix} \mathbf{U}_s \\ 0 \end{pmatrix} = \begin{pmatrix} \mathbf{R}_n & \mathbf{P}_m \\ \mathbf{P}_m^T & 0 \end{pmatrix} \begin{pmatrix} \mathbf{a} \\ \mathbf{b} \end{pmatrix} = \mathbf{G}\hat{\mathbf{a}}_s, \tag{31}$$

in which the matrix $\mathbf{G}$ is theoretically non-singular [45] and

$$\hat{\mathbf{a}}_s = \begin{pmatrix} \mathbf{a} \\ \mathbf{b} \end{pmatrix}. \tag{32}$$

Now from (31) we have

$$\hat{\mathbf{a}}_s = \mathbf{G}^{-1}\hat{\mathbf{U}}_s. \tag{33}$$

By rewriting Eq. (23) we obtain

$$u(\mathbf{x}) = \hat{\Phi}(\mathbf{x})\hat{\mathbf{U}}_s, \tag{34}$$

such that

$$\hat{\Phi}(\mathbf{x}) = [\mathbf{R}_n(\mathbf{x}), \mathbf{P}_m(\mathbf{x})]\mathbf{G}^{-1}. \tag{35}$$

The shape functions corresponding to the nodal displacements of radial point interpolation method (RPIM), are the first n functions of the above vector and we show them by the vector $\Phi^T(\mathbf{x})$, that means

$$\Phi(\mathbf{x}) = \{\phi_1(\mathbf{x}),\ \phi_2(\mathbf{x}),\ \ldots,\ \phi_n(\mathbf{x})\}. \tag{36}$$

Now Eq. (34) takes following form:

$$u(\mathbf{x}) = \Phi(\mathbf{x})\mathbf{U}_s = \sum_{i=1}^{n} \phi_i(\mathbf{x})u_i. \tag{37}$$

Also it is well known that the Kronecker delta function property is attached to the RPIM shape functions by (35) which is clarified, that means

$$\phi_i(\mathbf{x}_j) = \begin{cases} 1 & i = j,\ i, j = 1, 2, \ldots, n, \\ 0 & i \neq j,\ i, j = 1, 2, \ldots, n, \end{cases} \tag{38}$$

and lead to a sparse global collocation system. We assume that the total number of nodes that cover $\bar{\Omega} = \Omega \cap \partial\Omega$ is N. By rewriting Eq. (37), we have

$$u(\mathbf{x}) = \Phi(\mathbf{x})\mathbf{U}_s = \sum_{i=1}^{N} \phi_i(\mathbf{x})u_i. \tag{39}$$

Since, corresponding to node x_j, there is a shape function $\phi_i(\mathbf{x})$, $i = 1, 2, \ldots, N$, then obviously we have from Eq. (38) that

$$\forall x_j \in \Omega_x^c \quad \phi_i(x_j) = 0, \tag{40}$$

where $\Omega_x^c = \{x_j : \ x_j \notin \Omega_x\}$. Now the derivatives of $u(\mathbf{x})$ with respect to x_i, $i-$th component of $\mathbf{x} = \{x_1, \ldots, x_i, \ldots, x_N\}$, is determined as

$$\frac{\partial u}{\partial x_i}(\mathbf{x}) = \sum_{j=1}^{N} \frac{\partial \phi_j}{\partial x_i}(\mathbf{x}) u_j, \tag{41}$$

and for high derivatives of $u(\mathbf{x})$ we have

$$\frac{\partial^s u}{\partial (x_i)^s}(\mathbf{x}) = \sum_{j=1}^{N} \frac{\partial^s \phi_j}{\partial (x_i)^s}(\mathbf{x}) u_j, \tag{42}$$

where $\frac{\partial^s}{\partial (x_i)^s}$ is $s-$th derivatives with respect to x_i imply that due to Eq. (40), $\forall x_j \in \Omega_x^c$, $\frac{\partial^s \phi_j}{\partial (x_i)^s}(\mathbf{x}) = 0$, $s = 1, 2, \ldots$. Denoting $u_{x_i}^{(s)}(.) = \frac{\partial^s u(.)}{\partial (x_i)^s}$ and setting $x = x_i$ in Eq. (39), we get

$$\begin{pmatrix} u_{x_i}^{(s)}(\mathbf{x}_1) \\ \vdots \\ u_{x_i}^{(s)}(\mathbf{x}_N) \end{pmatrix} = \overbrace{\begin{pmatrix} \frac{\partial^s \phi_1}{\partial (x_i)^s}(\mathbf{x}_1) & \cdots & \frac{\partial^s \phi_N}{\partial (x_i)^s}(\mathbf{x}_1) \\ \vdots & \ddots & \vdots \\ \frac{\partial^s \phi_1}{\partial (x_i)^s}(\mathbf{x}_N) & \cdots & \frac{\partial^s \phi_N}{\partial (x_i)^s}(\mathbf{x}_N) \end{pmatrix}}^{D_{x_i}^s} \begin{pmatrix} u_1 \\ \vdots \\ u_N \end{pmatrix}. \tag{43}$$

This matrix-vector form for high-order derivatives is as follows:

$$U_{x_i}^s = D_{x_i}^s U, \tag{44}$$

where

$$U_{x_i}^s = \{u_{x_i}^{(s)}(\mathbf{x}_1), \ldots, u_{x_i}^{(s)}(\mathbf{x}_N)\}. \tag{45}$$

3 Implementation the method of lines for PIDEs

For any fixed value of $\mathbf{x}$, Eq. (1) is transformed into an ODE as follows:

$$\begin{aligned} \mathbf{y}_t(t, \mathbf{x}_i) &= \mathbf{f}(t, \mathbf{x}_i) + \nabla \cdot \mathbf{p}(t, \mathbf{x}_i), \\ \mathbf{p}(t, \mathbf{x}_i) &= \mathbf{A}(t, \mathbf{x}_i) \nabla \mathbf{y}(t, \mathbf{x}_i) - \int_0^t \mathbf{B}(t, s, \mathbf{x}_i) \nabla \mathbf{y}(s, \mathbf{x}_i) ds. \end{aligned} \tag{46}$$

Let $\sum_{k=1}^{N} \mathbf{y}_k(t) \phi_k(\mathbf{x})$ be the SMRPI approximation of $\mathbf{y}(t, \mathbf{x})$. By applying the GPS for (46) we will have:

$$\begin{aligned} \mathbf{y}_{j+1}(\mathbf{x}_i) &= \mathbf{y}_j(\mathbf{x}_i) + \eta_{i,j} \Big(\mathbf{f}(t_j, \mathbf{x}_i) + \nabla \cdot \mathbf{p}_j(\mathbf{x}_i) \Big), \\ \mathbf{p}_j(\mathbf{x}_i) &= \sum_{k=1}^{N} \Big(\mathbf{A}(t_j, \mathbf{x}_i) - \int_0^{t_j} \mathbf{B}(t_j, s, \mathbf{x}_i) ds \Big) \cdot \nabla \phi_k(\mathbf{x}_i) \mathbf{y}_j(\mathbf{x}_i), \end{aligned} \tag{47}$$

where $\mathbf{y}_j(\mathbf{x}_i)$ is equal to $\mathbf{y}_i(t_j)$ and estimates $\mathbf{y}(t,\mathbf{x})$ in $(t_j,\mathbf{x}_i)$. So, we have

$$\begin{aligned}\mathbf{y}_{i,j+1} &= \mathbf{y}_{i,j} + \eta_{i,j}\Big(\mathbf{f}(t_j,\mathbf{x}_i) + \nabla\cdot\mathbf{p}_{i,j}\Big),\\ \mathbf{p}_{i,j} &= \sum_{k=1}^{N}\Big(\mathbf{A}(t_j,\mathbf{x}_i) - \int_0^{t_j}\mathbf{B}(t_j,s,\mathbf{x}_i)ds\Big)\cdot\nabla\phi_k(\mathbf{x}_i)\mathbf{y}_{i,j},\end{aligned} \tag{48}$$

in which $\mathbf{y}_{i,j} = \mathbf{y}_j(\mathbf{x}_i)$.

4 Numerical results

For confirming our theoretical analysis, we need to consider a numerical example based on problem (1) with initial boundary conditions. The following symbols are introduced in order to analyze the error of this method:

$$|u-u_h|_0 = \Big[\int_\Omega |u-u_h|^2 d\Omega\Big]^{\frac{1}{2}}, \tag{49}$$

$$|u-u_h|_1 = \Big[\int_\Omega |\frac{\partial}{\partial x_1}(u-u_h)|^2 + |\frac{\partial}{\partial x_2}(u-u_h)|^2 d\Omega\Big]^{\frac{1}{2}}, \tag{50}$$

where u and u_h are the exact and the approximation solutions, respectively. To apply the SMRPI method for all examples, let $r_s = 4.5h$ that is significant enough to have sufficient number of nodes for any support domain in which used the radius of disks of support domain to construct basis functions. In Eq. (23) we use the thin plate spline with three order $\phi(\mathbf{x}) = \|\mathbf{x}\|^6\log\|\mathbf{x}\|$ where $\|.\|$ is the Euclidean norm in $\mathbb{R}^n$. Also, let $m = 21$ that causes the polynomial basis functions as following:

$$\begin{aligned}P_m^T(\mathbf{x}) = \{&1, x, y, x^2, xy, y^2, x^3, x^2y, xy^2, y^3, x^4, x^3y, x^2y^2,\\ &xy^3, y^4, x^5, x^4y, x^3y^2, x^2y^3, xy^4, y^5\}.\end{aligned}$$

In addition, all computations have been done with Mathematica software. To evaluate the benefits and validity of this method for solving problem (1), consider the following examples.

Example 1. Assume that $\mathbf{A}$ and $\mathbf{B}$ are identity matrices and the exact solution is

$$\mathbf{y}(t,\mathbf{x}) = \exp(-t)\sin(\pi x_1)\sin(\pi x_2),$$

on $\mathbf{x} = (x_1,x_2) \in \Omega = [0,1]^2$ and $t \in [0,1]$ with initial condition $g(\mathbf{x}) = 0$. Also, the associated forcing term $f(t,\mathbf{x})$ is determined by replacing the above functions into problem (1). Fig. 1 gives the associated error $y - y_N$

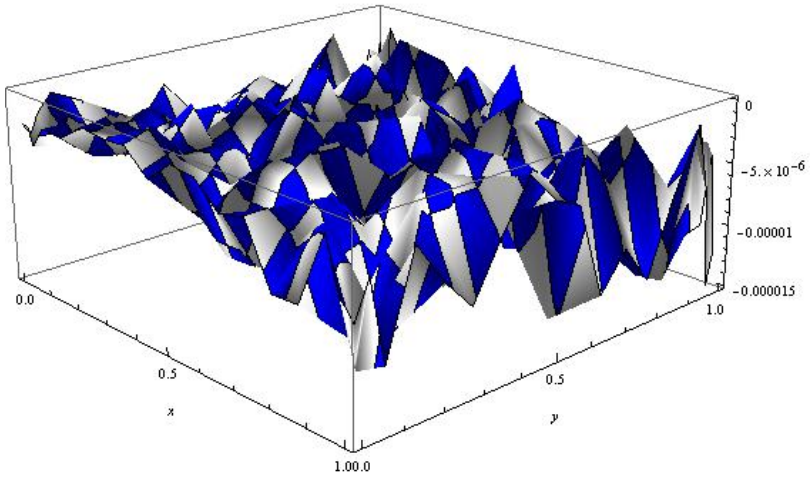

Figure 1: Error function $y - y_N$ with $h = 1/32$ and $N = 16$ for Example 1.

with $h = 1/32$. Error norms has been computed with different types of norms and the results have been presented in Table 1. From the presented results, it can be concluded that the accuracy of the numerical results have been improved by decreasing the number of h. In addition, this table states the effect of various values of the nodal spacing N on the results.

Example 2. Let

$$\mathbf{A}(t,\mathbf{x}) = \begin{pmatrix} 3+\|\mathbf{x}\|^2 & 1-\|\mathbf{x}\|^2 \\ 1-\|\mathbf{x}\|^2 & 4 \end{pmatrix},$$

and

$$\mathbf{B}(t,s,\mathbf{x}) = \begin{pmatrix} \exp(s+t) & 1 \\ 1 & t^2+s^2+4 \end{pmatrix}.$$

in which the initial condition is given by $g(\mathbf{x}) = 0$ and the exact solution is $\mathbf{y}(t,\mathbf{x}) = x_1x_2(1-x_1)(1-x_2)\sin(\pi t)$ in $\mathbf{x} = (x_1,x_2) \in \Omega = [0,1]^2$ and $t \in [0,1]$. So, the source function $f(t,\mathbf{x})$ is determined by embedding the above functions into problem (1). Fig. 2 gives the associated error $y - y_N$ with $h = 1/32$. The error norms have been computed with different types of norms and have been presented in Table 2. These numerical results clearly show the accuracy of this method.

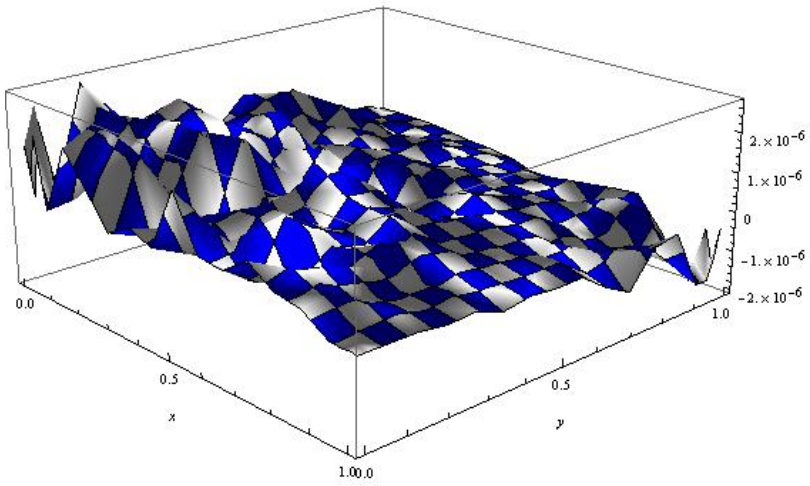

Figure 2: Error function $y - y_N$ with $h = 1/32$ and $N = 16$ for Example 2.

Table 1: Error norms for Example 1 with different values of N and h.

	$N = 8$			$N = 16$		
h	0.01	0.001	0.0001	0.01	0.001	0.0001
$-\log_{10}(\|y - y_N\|_0)$	2.4034	2.6843	2.9073	3.5320	3.8650	4.1058
$-\log_{10}(\|y - y_N\|_1)$	1.1034	1.3848	1.5931	2.1532	2.4860	2.7562

5 Conclusion

This paper has been devoted to solve parabolic integro-differential equations with mixed group preserving scheme and spectral meshless radial point interpolation by the method of lines. In spite of easy implementation of other methods for solving this problem, the challenge of these methods is their limited accuracy, locality, complexity and high cost of computing in linearization of the nonlinear terms. So, we have proposed the spectral meshless radial point interpolation scheme that, in addition employs radial functions as a means of local interpolation, offers a very flexible chart with a high accuracy for solving this parabolic equation. Numerical examples show that our suggested approach is more effective and accurate for various choices of norms and semi norms. Through this assessment, we are

Table 2: Error norms for Example 2 with different values of N and h.

		$N=8$			$N=16$		
	h	0.01	0.001	0.0001	0.01	0.001	0.0001
$-\log_{10}(\|y-y_N\|_0)$		2.5464	2.8011	3.0043	3.5532	3.7968	4.2625
$-\log_{10}(\|y-y_N\|_1)$		1.0034	1.3003	1.3883	2.3532	2.7560	2.8562

convinced that the described method is an effective numerical scheme for partial differential equations. More importantly, the proposed scheme is easy to implement and time saving. From the results which we can see in the tables and figures, it can be concluded that the spectral meshless radial point interpolation method has a good convergence characteristic. Interested readers are advised to apply this method for others partial differential equations.

References

[1] S. Abbasbandy, M.S. Hashemi and C.S. Liu, *The Lie-group shooting method for solving the Bratu equation*, Commun. Nonlinear Sci. Numer. Simul. **16**(11) (2011) 4238-4249.

[2] S. Abbasbandy and M.S. Hashemi, *Group preserving scheme for the Cauchy problem of the Laplace equation*, Eng. Anal. Bound. Elem., **35**(8) (2011) 1003-1009.

[3] I.H. Biswas, E.R. Jakobsen and K.H. Karlsen, *Difference-quadrature schemes for nonlinear degenerate parabolic integro-PDE*, SIAM J. Numer. Anal. **48**(3) (2010) 1110-1135.

[4] V. Capasso, *Asymptotic stability for an integro-differential reaction-diffusion system*, J. Math. Anal. Appl. **103**(2) (1984) 575-588.

[5] C. Chen, V. Thomee and L.B. Wahlbin, *Finite element approximation of a parabolic integro-differential equation with a weakly singular kernel*, Math. Comput. **58**(198) (1992) 587-602.

[6] C. Chang, C. Liu and J. Chang, *A group preserving scheme for inverse heat conduction problems*, Comput. Model. Eng. Sci. **10**(1) (2005) 13-27.

[7] H. Chen and D. Xu, *A compact difference scheme for an evolution equation with a weakly singular kernel*, Numer. Math. **5**(4) (2012) 559-572.

[8] Z. Chen and J. Zou, *Finite element methods and their convergence for elliptic and parabolic interface problems*, Numer. Math. **79**(2) (1998) 175-202.

[9] B. Deka and R.C. Deka, *Apriori $L^{\infty}(L^2)$ error estimates for finite element approximations to parabolic integro-differential equations with discontinuous coefficients*, Proc. Indian Nat. Sci. Acad. Math. Sci. **129**(49) (2019) 1129-1156.

[10] M. Dehghan and F. Shakeri, *Solution of parabolic integro-differential equations arising in heat conduction in materials with memory via He's variational iteration technique*, Int. J. Numer. Methods Biomed. Eng. **26**(6) (2010) 705-715.

[11] X. Da, *Finite element methods of the two nonlinear integro-differential equations*, Appl. Math. Comput. **58**(2-3)(1993) 241-273.

[12] R.E. Ewing, Y. Lin and J. Wang, *A numerical approximation of non-Fickian flows with mixing length growth in porous media*, E Acta Math. Univ. Comenian. (N.S.) **70** (2001) 75-84.

[13] W. Gao, M. Partohaghighi, H.M. Baskonus and S. Ghavi, *Regarding the group preserving scheme and method of line to the numerical simulations of Klein-Gordon model*, Results Phys. **15** (2019) 102-555.

[14] M.L. Heard, *An abstract parabolic Volterra integro-differential equation*, SIAM J. Numer. Anal. **13**(1) (1982) 81-105.

[15] M.S. Hashemi, E. Karatas and E. Darvishi, *Numerical treatment on one-dimensional hyperbolic telegraph equation by the method of line-group preserving scheme*, Eur. Phys. J. Plus. **134**(4) (2019) 153.

[16] C. Hongbin and C.C.X. Da, *A second order fully discrete difference scheme for a partial integro-differential equation*, Math. Numer. Sin. chinese edition **28**(2) (2006) 141.

[17] M. Kostoglou, *On the analytical separation of variables solution for a class of partial integro-differential equations*, Appl. Math. Lett. **18**(6) (2005) 707-712.

[18] S. Larsson, V. Thomee and L. Wahlbin, *Numerical solution of parabolic integro-differential equations by the discontinuous Galerkin method*, Math. Comput. **67**(221) (1998) 45-71.

[19] Y. Lin, *Galerkin methods for nonlinear parabolic integro-differential equations with nonlinear boundary conditions*, SIAM J. Numer. Anal. **27**(3) (1990) 608-621.

[20] Y.P. Lin, V. Thomee and L.B. Wahlbin, *Ritz-Volterra projections to finite-element spaces and applications to integro-differential and related equations*, SIAM J. Numer. Anal. **28**(4) (1991) 1047-1070.

[21] Y. Liu, Z. Fang, H. Li, S. He and W. Gao, *A new expanded mixed method for parabolic integro-differential equations*, Appl. Math. Comput. **259** (2015) 600-613.

[22] C. Liu, *A group preserving scheme for Burgers equation with very large Reynolds number*, Comput. Model. Eng. Sci. **12**(3) (2006) 197.

[23] C. Liu, *An efficient backward group preserving scheme for the backward in time Burgers equation*, Comput. Model. Eng. Sci. **12**(1) (2006) 55.

[24] C.S. Liu, *Group preserving scheme for backward heat conduction problems*, Int. J. Heat Mass. Transf. **47**(12-13) (2004) 2567-2576.

[25] C.S. Liu, *Cone of non-linear dynamical system and group preserving schemes*, Int. J. Non. Linear Mech. **36**(7) (2001) 1047-1068.

[26] C.S. Liu, *Solving an inverse Sturm-Liouville problem by a Lie-group method*, Bound. Value Probl. **1** (2008) 749-865.

[27] J.C. Lopez-Marcos, *A difference scheme for a nonlinear partial integro-differential equation*, SIAM J. Numer. Anal. **27**(1) (1990) 20-31.

[28] C.C. Miao and S. Tsimin, *Finite element methods for integro-differential equations*, (Vol. 9) World Scientific, 1998.

[29] C.A. Mnxeeb, *On the stability of multi-step finite-difference-based lattice Boltzmann schemes*, Int. J. Comput. Methods **15** (3) (2018) 1850-1887.

[30] K. Mustapha and H. Mustapha, *A second-order accurate numerical method for a semilinear integro-differential equation with a weakly singular kernel*, IMA J. Num. Anal. **30**(2) (2009) 555-578.

[31] K. Mustapha, H. Brunner, H. Mustapha and D. Schotzau, *An hp-version discontinuous Galerkin method for integro-differential equations of parabolic type*, SIAM J. Numer. Anal. **49**(4) (2011) 1369-1396.

[32] R.K. Miller, *An integro-differential equation for rigid heat conductors with memory*, J. Math. Anal. Appl. **66**(2) (1978) 313-332.

[33] A.K. Pani and T.E. Peterson, *Finite element methods with numerical quadrature for parabolic integro-differential equations*, SIAM J. Numer. Anal. **33**(3) (1996) 1084-1105.

[34] C.V. Pao, *Solution of a nonlinear integrodifferential system arising in nuclear reactor dynamics*, J. Math. Anal. Appl. **48**(2) (1974) 470-492.

[35] L. Qiao and D. Xu, *Compact alternating direction implicit scheme for integro-differential equations of parabolic type*, J. Sci. Comput. **76**(1) (2018) 565-582.

[36] G.M.M. Reddy, R.K. Sinha and J.A. Cuminato, *A posteriori error analysis of the Crank-Nicolson finite element method for parabolic integro-differential equations*, J. Sci. Comput. **79** (1) (2019) 414-441.

[37] R.K. Sinha, R.E. Ewing and R.D. Lazarov, *Mixed finite element approximations of parabolic integro-differential equations with nonsmooth initial data*, SIAM J. Numer. Anal. **47**(5) (2009) 3269-3292.

[38] R.K. Sinha, R.E. Ewing and R.D. Lazarov, *Some new error estimates of a semidiscrete finite volume element method for a parabolic integro-differential equation with nonsmooth initial data*, SIAM J. Numer. Anal. **43**(6) (2006) 2320-2343.

[39] E. Shivanian, *A new spectral meshless radial point interpolation (SMRPI) method: a well-behaved alternative to the meshless weak forms*, Eng. Anal. Bound. Elem. **54** (2015) 1-12.

[40] E. Shivanian, *Analysis of meshless local and spectral meshless radial point interpolation (MLRPI and SMRPI) on 3-D nonlinear wave equations*, Ocean Engineering **89** (2014) 173-188.

[41] E. Shivanian, *Spectral meshless radial point interpolation (SMRPI) method to two-dimensional fractional telegraph equation*, Math. Methods Appl. Sci. **39**(7)(2016) 1820-1835.

[42] E. Shivanian and A. Jafarabadi, *The spectral meshless radial point interpolation method for solving an inverse source problem of the time-fractional diffusion equation*, Appl. Numer. Math. **129** (2018) 1-25.

[43] T. Tang, *A finite difference scheme for partial integro-differential equations with a weakly singular kernel*, Appl. Numer. Math. **11**(4) (1993) 309-319.

[44] W. Wang and Q. Hong, *Two-grid economical algorithms for parabolic integro-differential equations with nonlinear memory*, Appl. Numer. Math. **142** (2019) 28-46.

[45] H. Wendland, *Error estimates for interpolation by compactly supported radial basis functions of minimal degree*, J. Approx. Theory. **93**(2) (1998) 258-272.

[46] E.G. Yanik and G. Fairweather, *Finite element methods for parabolic and hyperbolic partial integro-differential equations*, Nonlinear Anal. Theory Methods Appl. **12**(8) (1988) 785-809.

[47] R. Zacher, *Quasilinear parabolic integro-differential equations with nonlinear boundary conditions*, Differ. Integral Equ. **19**(10) (2006) 1129-1156.

[48] A. Zhu, T. Xu and Q. Xu, *Weak Galerkin finite element methods for linear parabolic integro-differential equations*, Numer. Methods Partial. Differ. Equ. **32**(5) (2016) 1357-1377.